SAND2000-1769J

Bifurcation Mode of Relativistic and Charge-Displacement Self-Channeling

A. B. Borisov[1], S. Cameron[2], T. S. Luk[2], T. R. Nelson[1,2], A. J. Van Tassle[1], J. Santoro[1], W. A. Schroeder[1], Y. Dai[1,3], J. W. Longworth[1,4], K. Boyer[1], and C. K. Rhodes[1]

[1] Department of Physics (M/C 273), University of Illinois at Chicago, Chicago, IL 60607-7059, *USA*

[2] Sandia National Laboratories, Albuquerque, NM 87185, *USA*

[3]Department of Mathematical and Computing Sciences, Tokyo Institute of Technology, O-Okayama, Meguro-ku, Tokyo 152-8552, *JAPAN*

[4]Department of Physics, Illinois Institute of Technology, Chicago, IL 60616, *USA*

ABSTRACT

Stable self-channeling of ultra-powerful (P_0 ~ 1 TW - 1 PW) laser pulses in dense plasmas is a key process for many applications requiring the controlled compression of power at high levels. Theoretical computations predict that the transition zone between the stable and highly unstable regimes of relativistic/charge-displacement self-channeling is well characterized by a form of weakly unstable behavior that involves bifurcation of the propagating energy into two powerful channels. Recent observations of channel instability with femtosecond 248 nm pulses reveal a mode of bifurcation that corresponds well to these theoretical predictions. It is further experimentally shown that the use of a suitable longitudinal gradient in the plasma density can eliminate this unstable behavior and restore the efficient formation of stable channels.

DISCLAIMER

DISCLAIMER

I. INTRODUCTION

Robust stability is known both theoretically [1-3] and experimentally [1-4] to be a chief characteristic of relativistic/charge-displacement self-channeling [1-12]. Moreover, it is known that the influence of the ponderomotively generated charge-displacement is the major factor [2] governing the stability of the confined modes of propagation and it has been observed that this feature has a counterpart in the ponderomotive stabilization present in related areas of plasma physics and accelerator design [2]. It is also theoretically clear [2,3] that the eigenmodes play a key role in the dynamics of the stability, since they function as attractors and efficiently guide the energy into stable states of high power compression.

A regime of unstable propagation is also theoretically predicted [2] to exist, although a systematic experimental study of its properties is lacking. The unstable behavior can be roughly classified into two subcategories. They are (1) strongly unstable propagation that results in catastrophic filamentation, an outcome associated with an operating point located deep in the unstable region [2], and (2) weak instability associated with the stable/unstable boundary zone in which deviations from stable single channel propagation initially become apparent. The former regime is characterized by the development of a group of peripheral small-scale filaments each containing a power on the order of the critical power for self-channeling. Under these circumstances, an increase in the incident laser power leads primarily to a disorganized multiplication of filaments with the outcome that the trapped power in an individual filament does not increase. In the case of weak instability, however, when typically two channels are formed, the power of the strongest channel can be raised with an increase of the incident laser power. Overall, the principal characteristics of the weakly unstable behavior are (a) bifurcation of the propagating mode and (b) the development of lateral displacements of the confined power.

The present study discusses these irregularities in the propagation by examining both their experimental observation and the corresponding theoretical description. The main findings reported in this work are (i) the first experimental observations of bifurcation of the propagating channel and (ii) experimental confirmation of the previously proposed [1] use of a suitable longitudinal gradient in the plasma density for both the restoration of stable propagation and channel optimization.

II. DISCUSSION OF RESULTS

Experimental evidence for bifurcation is shown in Fig. 1(a), an image that displays a transverse view of the spectrally integrated Xe(M) radiation (~1keV) produced by the propagating ultraviolet (248nm) radiation in a gaseous xenon cluster target [4,5] having a Xe density of ~ 3×10^{19} cm^{-3}. The methods of measurement and the experimental conditions generally pertaining to the data in Fig. 1(a) have been previously described [4]. An interpretation of the observed Xe(M) spectrum has also been given [13].

The key feature shown in Fig. 1(a) is the dual structure visible at the longitudinal position $z \cong 1500$ μm. Since x-rays are generated, this indicates the existence of two separate parallel zones in which the power is highly compressed. In contrast, at the position corresponding to $z \cong 600$ μm, only a single feature is evident. In the process of channel formation, the incident propagating energy collapses from this initial region to a thin channel whose volume is sufficiently small that the x-ray emission from it is not visible in the exposure on account of the detection limit imposed by combined influence of (i) the relatively low spatial resolution (~ 30 μm), (ii) the bound on the dynamic range of the detector, and (iii) the quenching of the Xe(M) emission in the high intensity zone of the channel that is caused by stripping of the entire 3d-shell by field ionization. This behavior causes the longitudinal gap (800 μm $\leq$ z $\leq$ 1400 μm) in the x-ray emission to occur. The subsequent bifurcation of the thin (~2-3 μm radius) channel [1-3] causes the dual feature at $z \cong 1500$ μm to appear. We note that other studies [14] have examined the spectral properties of the Xe(L) emission from the intense central region of the filament.

The observed morphology of the x-ray signal can be put in contact with computations of the dynamics for conditions corresponding to those of the experiment. The modeling of the relativistic/charge-displacement self-channeling is based on a relatively simple model [5,6] that involves two dimensionless parameters; one represents the normalized power η, while the other describes the normalized radius ρ_0 of the incident radiation. They are given respectively by

$$\eta = P_0 / P_{cr} \qquad \text{and} \qquad \rho_0 = r_0 \omega_{p,0} / c . \tag{1}$$

In Eq. (1) P_0 represents the incident peak power associated with the central zone of the pulse and P_{cr} denotes the critical power for relativistic/charge-displacement self-channeling given by [5-7]

$$P_{cr} = (m_{e,0}^2 c^5 / e^2) \int_0^\infty g_0^2(\rho) \rho d\rho \, (\omega / \omega_{p,0})^2 = 1.6198 \text{x} 10^{10} \, (\omega / \omega_{p,0})^2 \, \text{W} , \tag{2}$$

in which $m_{e,0}$, c, and e have their standard identifications, $g_0(\rho)$ is the Townes mode [15], and ω, $\omega_{p,0} = (4\pi e^2 N_{e,0} / m_{e,0})^{1/2}$, and r_0, respectively denote the angular frequency corresponding to the propagating radiation, the angular frequency of the unperturbed plasma, and the radius of the incident transverse intensity profile. A chief feature of the self-channeling process is the stabilization of the transverse beam profile near one of the z-independent modes of propagation designated as the lowest eigenmodes [5,6] $U_{s,0}(\rho)$ (with index s, $0 < s < 1$) of the governing nonlinear Schrödinger equation. These eigenmodes have the dimensionless radius

$$\rho_{e,0} \equiv [2\int_0^\infty U_{s,0}^2(\rho)d\rho / U_{s,0}^2(0)]^{1/2}. \tag{3}$$

The self-channeling process can be described as the dynamic adjustment of the radius r_0 of the incident focused beam to the radius r_{ch} of the laser channel, the value of which can be derived from the dimensionless radius $\rho_{e,0}$ of the corresponding lowest eigenmode [3,6] as

$$r_{ch} = \frac{c\rho_{e,0}}{\omega_p}. \tag{4}$$

Previous analysis [6] has shown that in the case of relativistic and charge-displacement self-channeling, the dimensionless radius of the channel $\rho_{e,0}$ varies extremely slowly over a large range of normalized laser power η, $\rho_{e,0} \approx$ const for $\eta > 1.5$, a property evident in Fig. 2. Therefore, from the expression for the plasma frequency

$$\omega_p = (3\pi e^2 N_e / m_{e,0})^{1/2}, \tag{5}$$

we conclude that the radius of the laser channel formed in a plasma with a local electron density N_e scales in good approximation [3] simply as

$$r_{ch} \sim N_e^{-1/2}. \tag{6}$$

The situation involving $\eta = P_0 / P_{cr} \gg 1$ and $r_0 / r_{ch} \gg 1$ leads to a strong self-focusing response which can be either stable or unstable [1,2]. Unfortunately, even in the stable case, the propagation is generally characterizing by a substantial loss of laser power and the efficiency of the process is grossly compromised [3]. However, the efficiency of the power compression can be optimized when $r_0 \sim r_{ch}$ (or, equivalently, $\rho_0 \sim \rho_{e,0}$), a condition that can be dynamically achieved by the adjustment of the local electron density N_e (see Eq. (6)). This can be readily achieved with the use of an appropriate longitudinal gradient in the electron density distribution [3].

Previous work [2] has shown that the conditions governing the stability of relativistic/ponderomotive self-channeling are well described by two-dimensional (η,ρ_0) stability maps of the form illustrated in Fig. (2) and that specific zones corresponding to stable and strongly unstable propagation can be identified. In particular, the stability and efficiency of the relativistic/charge-displacement self-channeling mechanism have been analyzed [1,2] for perturbed Gaussian beams having incident transverse amplitude distributions given by

$$U_0(r,\phi) = I_0^{1/2} \exp(-0.5(r/r_0)^2 \times (1 + (r/r_0)^4 \sum \epsilon_q \cos(q\phi)). \tag{7}$$

In the profile represented by Eq. (7), the weak azimuthal perturbations are characterized by

$$\epsilon_q = 0.03, \quad q = 1-4, \quad \delta = \max|I_0(r,\phi_1) - I_0(r,\phi_2)|/I_0 = 0.21. \qquad (8)$$

The information presented in the stability (η, ρ_0) map illustrated in Fig. (2) can be used to establish a direct correspondence between the experimental data shown in Fig. 1(a) and the theoretical procedures applicable to the dynamics of pulses with amplitude distributions given generally by the form of Eq. (7). The gaseous xenon cluster target is experimentally [4,14] produced by a pulsed valve having a ~ 1.5 mm orifice that is equipped with a vertical barrier on the side facing the incident 248nm beam. This wall, which contains an aperture having a diameter of ~100 μm, blocks the lateral expansion of the gas except in the local zone near the ~100 μm opening. Accordingly, a focal position located sufficiently inside the wall corresponds well to a uniform target density. In contrast, location of the focus in the region near or slightly outside of the 100 μm aperture causes the focussed pulse to propagate through a zone in which a substantial longitudinal gradient in target density is present. Therefore, adjustment of the focal position along the direction of propagation in the region defined by the barrier enables the alteration of the density gradient experienced by the focussed radiation. Consequently, there exists a controllable experimental procedure that can provide either a uniform target density or one possessing an appreciable density gradient.

The ability to modify the longitudinal density profile enables the dynamic trajectory of the operating point [1,3] of the system to be grossly altered. The principal consequence of this control, for the data shown in Fig. 1(a), can be understood by reference to Fig. 1(b) and Fig. (2). The initial condition corresponding to the development of the experimentally observed bifurcated channel illustrated in Fig. 1(a) is designated by the datum $A_{uniform}$ in Fig.(2), a point that lies near the zone in which strong filamentation occurs [2]. Although in the stable region, it is significant to note that $A_{uniform}$ is clearly located at a considerable remove from the eigenmode curve of the system $\rho_{e,o}(\eta)$ in this situation.

The computed evolution of an incident pulse corresponding to $A_{uniform}$ is illustrated in Fig. 1(b). The salient feature of the theoretical distribution is a strong spatial bifurcation, a characteristic that is in good qualitative correspondence with the experimental observation shown in Fig. 1(a). Indeed, bifurcation into two roughly equal channels is shown. Experimentally, the bifurcated propagation becomes visible when the divergence of the two channels is sufficiently great that they can be separately resolved by the x-ray camera [4]. A continuation of the computed evolution of the pulse to longitudinal distances Z > 400 μm reveals that the stronger component of the bifurcated distribution shown in Fig. 1(b) forms a stable channel that is denoted by point $B_{uniform}$ in Fig.(2). We note that this datum falls very close to the eigenmode curve $[\rho_{c,o}(\eta)]$, a basic property of fully evolved stable channels [1,3] and a sharp contrast to the initial condition given by the location of $A_{uniform}$.

Previous studies have demonstrated that stable channels aggressively seek the eigenmode distribution [6]. Hence, the existence of a channel with an operating point corresponding to a position far from the eigenmode curve necessitates a major reorganization of its structure. The present results indicate that, for circumstances requiring a sufficiently large adjustment, the process of bifurcation enables the operating point of the system to make a single large and abrupt step toward the eigenmode curve. This mechanism, however, leads to very high losses, as the relative positions of $A_{uniform}$ and $B_{uniform}$ in Fig. (2) illustrate.

The use of a plasma gradient greatly alters the dynamics of propagation [3]. Specifically, it was theoretically predicated [3] that the process of bifurcation could be eliminated by the use of a suitable plasma gradient. This predication has now been experimentally confirmed, as shown by the data presented in Fig. 3(a). The morphology of the channel seen in Fig. 1(a) is transformed into that shown in Fig. 3(a) by a relocation of the incident focal zone to a region possessing an appreciable density gradient. It is apparent that the bifurcated region ($z \cong 1500$ μm) of the former has been replaced by an intense single channel in the latter. This was achieved experimentally solely by a small longitudinal shift in the focal position of the incident pulse to the region near the 100 μm aperture where a significant gradient in the target density exists. This adjustment places the operating point of the incident radiation in the proximity of the eigenmode.

A corresponding calculation of the pulse evolution which includes a suitable density gradient, shown in Fig. 3(b), illustrates the smooth development of a single channel. In this case, the initial condition has been remapped to point $A_{gradient}$ in Fig. (2) and the trajectory of the operating point leads to the stable configuration by $B_{gradient}$. Since the loss caused by the formation of the second subsidiary channel in the bifurcated case has been eliminated, the efficiency of the transport into the channel formed has been significantly increased. The existence of the plasma gradient enables the pulse to reorganize in a less abrupt manner, thereby eliminating the need for the bifurcation.

III. CONCLUSIONS

Experimental observations of channel instability show good correspondence to computations of the channel dynamics. The leading instability is seen to be bifurcation of the propagating mode. The use of an appropriate density gradient can control this instability and lead to the efficient development of stable channels.

ACKNOWLEDGEMENTS

Support for this research was provided under contracts with ARO (DAAH04-94-G-0089), ARO (DAAG55-97-1-0310), the Japanese Ministry of Education, Science, Sport, and Culture and the Department of Energy at the Sandia National Laboratories. Sandia is a multiprogram laboratory operated by Sandia Corporation, a Lockheed Martin Company, for the United States Department of Energy under contract DE-AC04-94AL85000.

FIGURE CAPTIONS

Figure 1:

(a) Experimentally observed morphology of channeled propagation obtained by imaging the Xe(M) radiation (~ 1keV) transverse to the channel with an x-ray pinhole camera having a spatial resolution of ~ 30 μm. The procedures of the measurement are described in Ref. [4}. The incident 248 nm pulse had an energy of ~ 350 mJ and a pulse width of ~ 270fs. The initial focusing action begins at $z \cong 0.5$ mm and a clearly bifurcated region is visible at $z \cong 1.5$ mm. See text for discussion.

(b) Computed pulse evolution corresponding to the experimental circumstances yielding the observed pattern shown in Fig. 1 (a). A strong bifurcation of the propagating node is seen, an outcome matching the experimental result.

Figure 2:

Stability map with coordinates (η, ρ_0). The eigenmode curve, $\rho_{e,0}(\eta)$ is shown. A full description appears in Ref. [1]. See text for discussion of designated loci.

Figure 3:

(a) Morphology of channel seen with adjustment of the incident focal volume to a region having an appreciable longitudinal plasma density gradient. The procedures of measurement were identical to those used in Fig. 1(a). A single channel is seen. See text for discussion.

(b) Computed channel evolution for a pulse corresponding to the experimental conditions yielding the result in Fig. 3(a). A single channel is observed in conformance with observation.

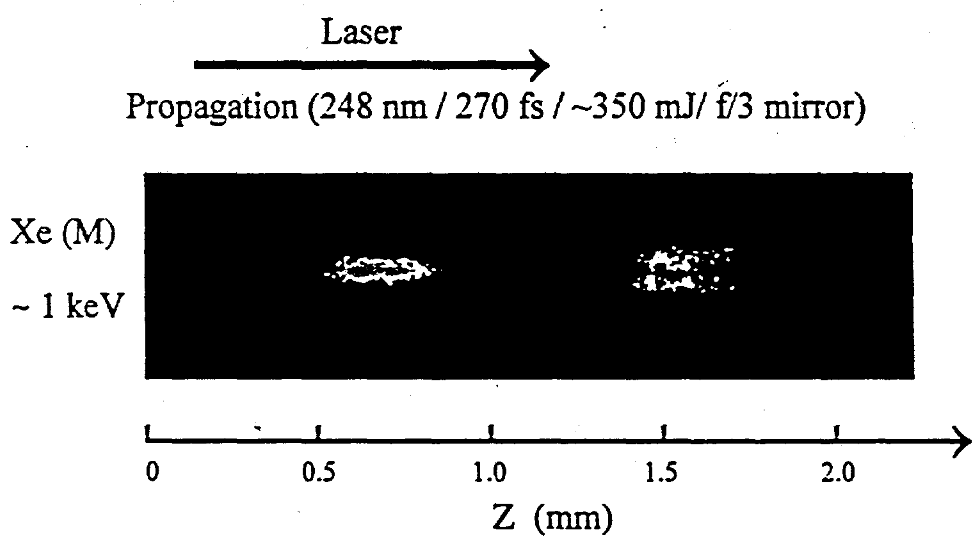
Laser
Propagation (248 nm / 270 fs / ~350 mJ/ f/3 mirror)
Xe (M)
~ 1 keV
0
0.5
1.0
1.5
2.0
Z (mm)

Fig. 1(a)

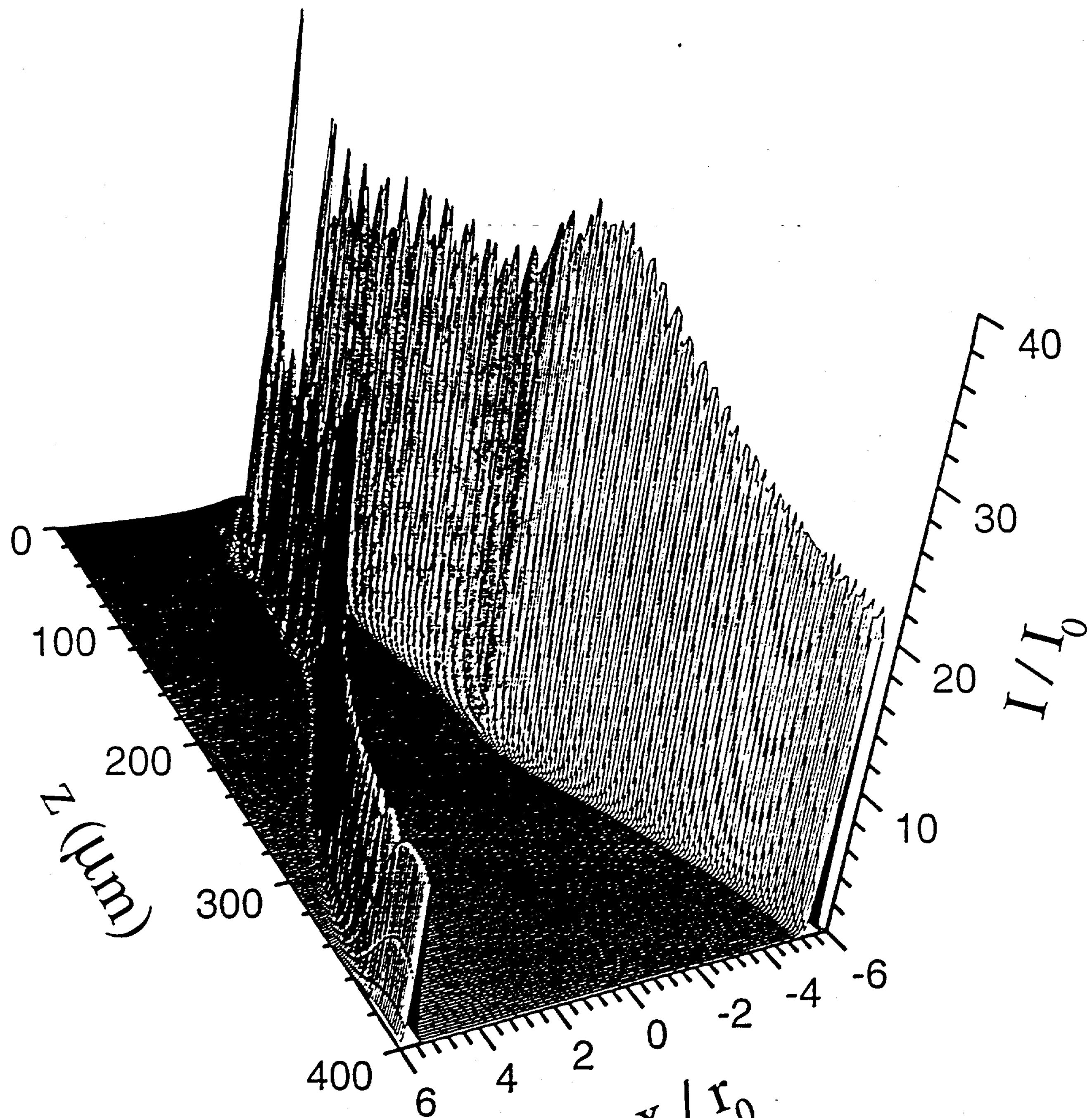

Fig. 1(b)

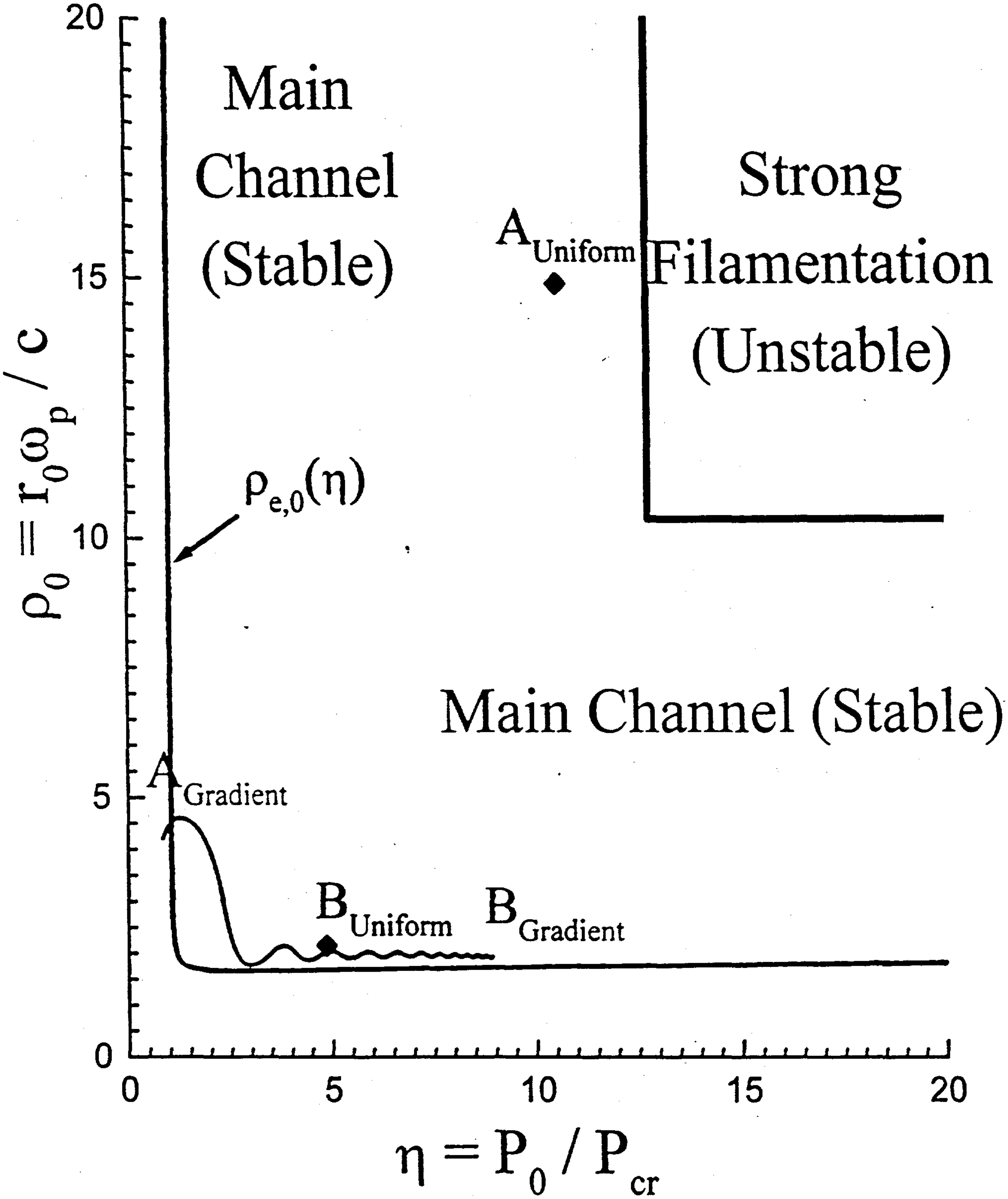
Main Channel (Stable)
Strong Filamentation (Unstable)
$A_{Uniform}$
$\rho_{e,0}(\eta)$
Main Channel (Stable)
$A_{Gradient}$
$B_{Uniform}$
$B_{Gradient}$
$\rho_0 = r_0\omega_p / c$
$\eta = P_0 / P_{cr}$
0
5
10
15
20

Fig. 2

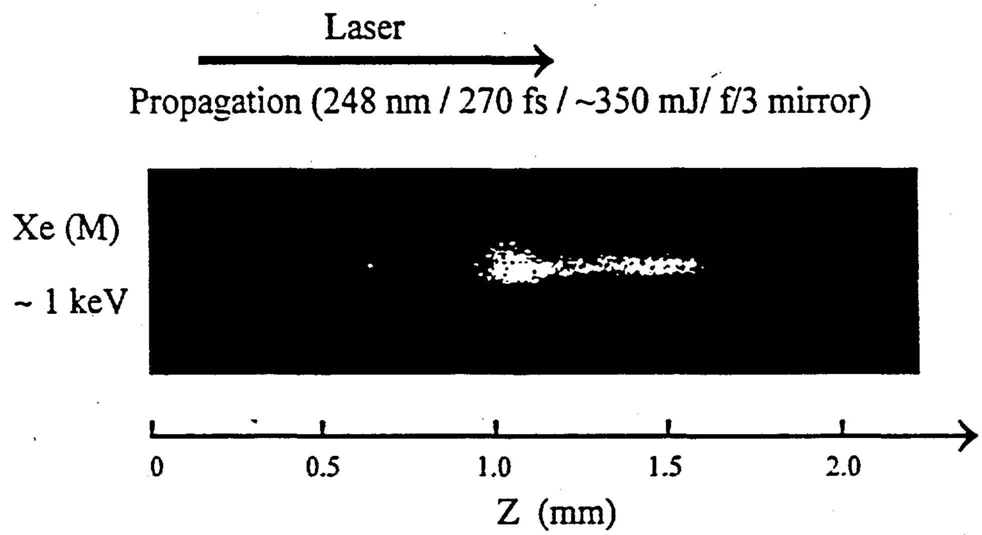
Laser
Propagation (248 nm / 270 fs / ~350 mJ/ f/3 mirror)
Xe (M)
~ 1 keV
0
0.5
1.0
1.5
2.0
Z (mm)

Fig. 3(a)

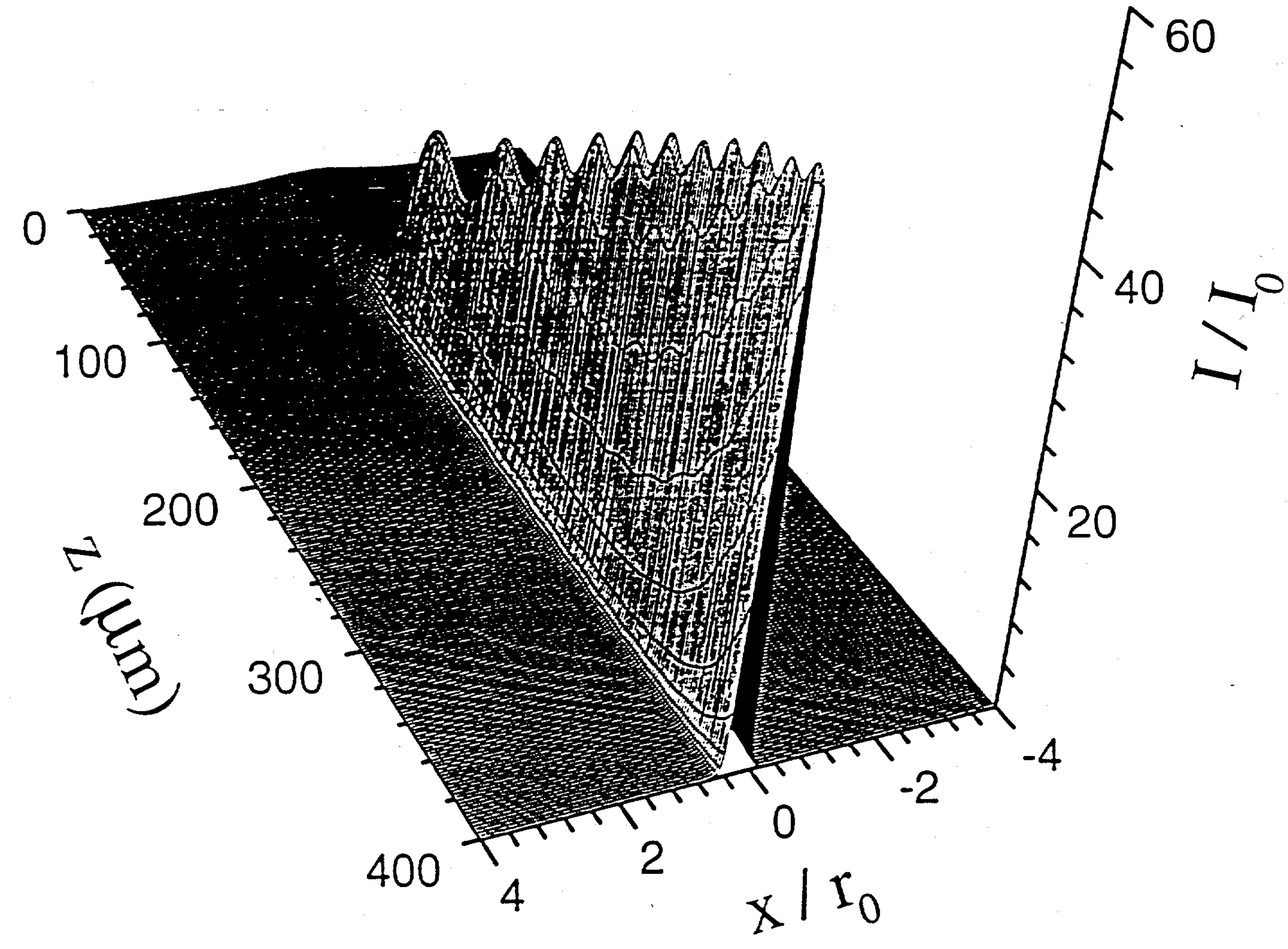

Fig. 3(b)

REFERENCES

1. Borisov, A. B., Longworth, J. W., Boyer, K., and Rhodes, C. K., "Stable Relativistic/Charge-Displacement Channels In Ultrahigh Power Density (~10^{21} W/cm^{3}) Plasmas," *Proc. Acad. Sci. USA* **95**, 7854, (1998).

2. Borisov, A. B., Shiryaev, O. B., McPherso,n A., Boyer K., and Rhodes, C. K, "Stability Analysis of Relativistic and Charge-Displacement Self-Channeling of Intense Laser Pulses In Underdense Plasmas," *Plasma Phys. Control. Fusion* **37**, 56 (1995).

3. Borisov, A. B., Cameron, S., Dai, Y., Davis, J., Nelso,n T., Schroeder, W. A., Longworth, J. W., Boyer, K., and Rhodes, C. K., "Dynamics of Optimized Stable Channel Formation of Intense Laser Pulses with the Relativistic/Charge-Displacement Mechanism," *J. Phys. B* **32**, 3511 (1999).

4. Borisov, A. B., McPherson, A., Thompson, B. D., Boyer, K., and Rhodes, C. K., "Ultrahigh Power Compression for X-Ray Amplification: Multiphoton Cluster Excitation Combined with Non-Linear Channeled Propagation," *J. Phys. B* **28**, 2143 (1995).

5. Sun, G-Z., Ott E., Lee, Y. C., and Guzdar, P., "Self-Focusing of Short Intense Pulses in Plasmas," *Phys. Fluids* **20**, 526 (1987).

6. Borisov, A. B., Borovskiy, A. V., Shiryaev, O. B., Korobkin, V. V., Prokhorov, A. M., Solem, J. C., Luk, T. S., Boyer, K., and Rhodes, C. K., "Relativistic and Charge-Displacement Self-Channeling of Intense Ultrashort Laser Pulses in Plasmas," *Phys. Rev. A* **45**, 5830 (1992).

7. Borisov, A. B., Borovskiy, A. V., Korobkin, V. V., Prokhorov, A. M., Shiryaev, O. B., Shi, X. M., Luk, T. S., McPherson, A., Solem, J. C., Boyer, K., and Rhodes, C. K., "Observation of Relativistic and Charge-Displacement Self-Channeling of Intense Subpicosecond Ultraviolet (248 nm) Radiation in Plasmas," *Phys. Rev. Lett.* **68**, 2309 (1992).

8. Borisov, A. B., Shi, X. M., Karpov, V. B., Korobkin, V. V., Shiryaev, O. B., Solem, J. C., McPherson, A., Boyer, K., and Rhodes, C. K., "Stable Self-Channeling of Intense Ultraviolet Pulses in Underdense Plasma, Producing Channels Exceeding 100 Rayleigh Lengths," *J. Opt. Soc. Am. B* **11**, 1941 (1994).

9. Monot, P., Auguste, T., Gibbon, P., Jakober F., Mainfray, G., Dulieu, A., Louis-Jacquet, M., Malka, G., and Miquel, J. L., "Experimental Demonstration of Relativistic Self-Channeling of a Multiterawatt Laser Pulse in an Underdense Plasma," *Phys. Rev. Lett.* **74**, 2953 (1995).

10. Wagner, R., Chen, S-Y., Maksimchuk, A., and Umstadter, D., Electron Acceleration by a Laser Wakefield in a Relativistically Self-Guided Channel," *Phys. Rev. Lett.* **78**, 3125, (1997).

11. Feit, M. D., Garrison, J. C., and Rubenchik, A. M., "Channeling of Intense Laser Beams in Underdense Plasmas," *Phys. Rev. E* **56**, 2394, 1997.

12. Chen, S-Y., Sarkisov, G. S., Maksimchuk, A., Wagner, R., and Umstadter, D., "Evolution of a Plasma Waveguide Created during Relativistic-Ponderomotive Self-Channeling of an Intense Laser Pulse," *Phys. Rev. Lett.* **80**, 2610 (1998).

13. Borisov, A. B., Longworth, J. W., McPherson, A., Boyer K., and Rhodes, C. K., "Dynamical Orbital Collapse Drives Super X-ray Emission," *J. Phys. B* **29**, 247 (1996).

14. Borisov, A. B., McPherson, A., Boyer, K., and Rhodes, C. K., "Z-Imaging of Xe(M) and Xe(L) Emissions from Channeled Propagation of Intense Femtosecond 248 nm Pulses in a Xe Cluster Target," *J. Phys. B: At. Mol. Opt. Phys.* **29**, L113 (1996).

15. Chiao, R. Y., Garmire, E., and Townes, C. H., "Self-Trapping of Optical Beams," *Phys. Rev. Lett.* **13**, 479 (1964).

16. Bespalov, V. I. and Talanov, V. I., "Filamentary Structure of Light Beams in Nonlinear Liquids," *Pis'ma Zh. Eksp. Teor. Fiz.* **3**, 471 (1966), [*JETP Lett.* **3**, 307 (1966)].

17. Campillo, A. J., Shapiro, S. L., and Suydam B. R., "Periodic Breakup of Optical Beams Due to Self-Focusing," *Appl. Phys. Lett.* **23**, 628 (1973).